CircHECTD1 mediates pulmonary fibroblast activation *via* HECTD1

Ther Adv Chronic Dis

2019, Vol. 10: 1–18

DOI: 10.1177/2040622319891558

Han Chu, Wei Wang, Wei Luo, Wei Zhang, Yusi Cheng, Jie Huang, Jing Wang, Xiaoniu Dai, Shencun Fang and Jie Chao

Abstract

Background: Circular RNA (circRNA), a new class of noncoding RNA, has been shown to be important in silicosis due to its unique role as a transcription regulator or as a sponge of small RNA regulators. Here, the mechanisms underlying circHECTD1/HECTD1 in fibroblast activation and subsequent fibrosis induced by SiO_2 were investigated.

Methods: Primary human pulmonary fibroblasts (HPF-a) were utilized, combined with quantitative real-time PCR (qRT-PCR) and fluorescence in situ hybridization (FISH) assays. LC3B-LV-RFP lentivirus was used to evaluate the role of autophagy. The CRISPR/Cas9 system was applied to specifically knock down HECTD1, combined with MTT, BrdU, and migration assays, to explore the functional changes induced by SiO_2.

Results: After exposure to SiO_2, the circHECTD1 level was decreased, which was associated with an increase in HECTD1 in HPF-a cells. SiO_2-induced autophagy was reversed by either circHECTD1 overexpression or HECTD1 knockdown in HPF-a cells, with restored SiO_2-induced fibroblast activation, proliferation, and migration *via* downstream autophagy. The lungs of mice exposed to SiO_2 confirmed the upregulation of HECTD1 in pulmonary fibroblasts.

Conclusions: Our data suggested a link between circHECTD1/HECTD1 and fibroblast activation with subsequent fibrosis induced by SiO_2, providing novel insight into the potential of circHECTD1/HECTD1 to be a therapeutic target for silicosis.

Keywords: activation, circRNA, HECTD1, migration, proliferation, silicosis

Received: 13 July 2019; revised manuscript accepted: 4 November 2019.

Correspondence to:
Jie Chao
Department of Physiology, School of Medicine, Southeast University, 87 Dingjiaqiao Road, Nanjing, Jiangsu, 210009, China

Department of Respiration, Zhongda Hospital, School of Medicine, Southeast University, Nanjing, Jiangsu, 210009, China

Key Laboratory of Developmental Genes and Human Disease, Southeast University, Nanjing, Jiangsu, 210096, China

Department of Respiratory Medicine, Nanjing Chest Hospital, Nanjing, Jiangsu, 210029, China
chaojie@seu.edu.cn

Han Chu
Department of Physiology, School of Medicine, Southeast University, Nanjing, Jiangsu, China

Department of Respiration, Zhongda Hospital, School of Medicine, Southeast University, Nanjing, Jiangsu, China

Key Laboratory of Developmental Genes and Human Disease, Southeast University, Nanjing, Jiangsu, China

Department of Respiratory Medicine, Nanjing Chest Hospital, Nanjing, Jiangsu, China

Wei Wang
Shencun Fang
Department of Respiratory Medicine, Nanjing Chest Hospital, Nanjing, Jiangsu, China

Wei Luo
Wei Zhang
Yusi Cheng
Jie Huang
Jing Wang
Xiaoniu Dai
Department of Physiology, School of Medicine, Southeast University, Nanjing, Jiangsu, China

Introduction

Silicosis is a pulmonary fibrosis disease caused by the long-term inhalation of free SiO_2. As a serious occupational disease, silicosis has a very high morbidity rate and thus attracts much attention in the public health field.[1–3] There are two main problems in the treatment of silicosis. First, there is no specific target for screening diagnosis in the early stage. Once diagnosed, it is already in the late stage of irreversible fibrosis, and effective treatment for pulmonary fibrosis in the late stage is lacking.[4] The pathophysiology of silicosis starts with phagocytosis of silica in macrophages, which causes an inflammatory cascade that leads to excessive fibroblast proliferation and migration, and gradually forms fibrosis.[5,6] Despite numerous studies that have been conducted to explore the toxicity of crystalline silica, the specific mechanism underlying silicosis is not well understood.[7]

Our recent studies suggest that autophagy, an evolutionarily conserved and catabolically driven cytoprotective process, plays a major role in determining cellular fate in silicosis.[8–10] Autophagy contributes to the removal of harmful cytoplasmic substances, and damaged organelles allow cells to mitigate various types of cellular stress.[11,12] Furthermore, autophagy participates in development, cellular homeostasis, and pathological processes, and even promotes cell survival. Plenty of evidence suggests that silica nanoparticles will be phagocytosed by autophagosomes, and indicates

that the dysregulation of autophagy may contribute to granuloma development and progression in silicosis[13]; however, the specific relationship between autophagy and silicosis remains unclear.[14,15] While the role of autophagy in macrophages after SiO_2 exposure has been confirmed,[16] whether autophagy is also involved in the pathogenetic process of fibroblasts after silica exposure needs to be elucidated.

Interestingly, the mechanisms involved in the regulation of autophagy are complicated, although circular RNAs (circRNAs), a type of widespread and diverse noncoding RNA, have been shown to play a specific role in the inflammation induced by silica. circRNAs are known to be involved in the processes of some human diseases.[17–19] For example, circRNAs can competitively bind with miRNAs, and, as a result, have been identified as sponges for miRNAs.[20] Some reports suggest that circRNAs regulate the cell cycle process and enhance the expression of parent genes; even a portion of circRNAs can be translated to generate functional proteins.[21–23] Given that circRNAs play fundamental roles in various cellular processes, we believe that circRNAs will contribute greatly toward facilitating research on the process of pulmonary fibrosis and even the treatment of silicosis.

Domain-containing E3 ubiquitin protein ligase 1 (HECTD1) is widely expressed in a range of human and murine primary cells and cell lines, including macrophages, neuronal cells and insulin secreting β-cells.[24,25] According to previous studies, HECTD1 is involved in the epithelial to mesenchymal transition (EMT), cell migration and various cellular processes.[26–28] Furthermore, HECTD1 was found to be related to MCPIP1, a deubiquitinase that plays a crucial role in fibrosis induced by silica.[7,10] In this study, circHECTD1 and HECTD1 both affected fibroblast activation and proliferation and cell migration. These results suggest that circHECTD1 and HECTD1 participate in regulating the process of pulmonary fibrosis and silicosis.

Materials and methods

Reagents

Regarding the SiO_2 particles, approximately 80% had a diameter between 1 and 5 μm; they were purchased from Sigma-Aldrich (S5631; Billerica, MA, USA), selected *via* sedimentation according to Stokes' law, acid-hydrolyzed, and baked overnight (200°C, at least 16 h). The silica samples were used for the *in vitro* continuous treatment cell experiments and suspended in normal saline (NS) at a concentration of 5 mg/ml, and the dose applied was 50 μg/cm^2, which was 20 μl/well in a 24-well plate. Primary antibodies against HECTD1 (sc-134976, rabbit polyclonal antibody) and vimentin (sc-7558, goat polyclonal antibody) were purchased from Santa Cruz Biotechnology®, Inc. (Dallas, TX, USA). Antibodies against GAPDH (MB001, Mouse) were obtained from Bioworld, Inc. (Louis Park, MN, USA).

Establishment of a mouse model of silicosis

Male C57BL/6 mice (22–30 g) were obtained from Nanjing Medical University Laboratories (Nanjing, China), and maintained on a 12:12 h light/dark cycle under constant temperature (23°C) and humidity (50%) conditions with free access to food and water. Animals were anesthetized with an intraperitoneal injection of pentobarbital sodium, and their tracheae were surgically exposed. A prepared SiO_2 suspension (0.2 g/kg in 50 mg/ml saline) was instilled intratracheally in one dose. Control animals were administered the same volume of sterile saline, as previously described.[9] Lung tissues were collected 28 days after treatment after an overdose of isoflurane to anesthetize the animal, followed by a pneumothorax and perfusion. The pulmonary tissues were dehydrated with 30% sucrose solution, and fixed with 4% formalin before being stained. All animal procedures were performed in strict accordance with the ARRIVE guidelines, and the animal protocols were approved by the Institutional Animal Care and Use Committee of the Medical School of Southeast University.

Cell culture

Human pulmonary fibroblasts from adults (HPF-a) were purchased from ScienCell and cultured in DMEM supplemented with 10% FBS, 100 U/ml penicillin, 100 μg/ml streptomycin, and 2 mM L-GlutaMAX (Gibco) at 37°C in a humidified 5% CO_2 atmosphere. To conduct experiments, we seeded cells in 24-well plates at a concentration of 1×10^5 cells/ml for 24 h before further treatment. The cell concentration was adjusted according to the requirements of the specific experiments.

Lentiviral transfection

P3-4 HPF-a cells were transfected with LV-RFP lentivirus (HANBIO Inc., Shanghai, China) as previously described.[16] Briefly, HPF-a cells (1×10^4 cells/well) were seeded in a 24-well plate for 48 h. After replacement with fresh medium containing 8 μg/ml polybrene, the cells were incubated with 100 μl of lentivirus solution (10^7 IU/ml) for 24 h. Then, the medium was replaced with fresh DMEM containing 10% FBS until the cells reached >50% confluence. To purify the GFP-labeled cells, blasticidin was added to medium containing 10 μg/ml puromycin and 10% FBS for culture for 24 h. Then, the cells were washed twice with fresh medium. Purified transduced HPF-a cell cultures were expanded and stored in liquid nitrogen as described previously.[16]

Western blotting

Western blotting was performed to determine the expression levels of specific proteins in HPF-a cells according to a standard protocol. Blots were imaged using a Tanon® scanner. Briefly, HPF-a cells were cultured in 24-well plates. After the cells were treated, they were washed twice with precooled PBS, and the cells were harvested using cell lysis solution containing proteinase inhibitors (100:1). The concentrations of proteins were balanced by the BCA assay according to the manufacturer's protocol (Beyotime). The proteins were separated by sodium dodecyl sulfate polyacrylamide gel electrophoresis and then transferred to PVDF membranes. The membranes were blocked with 5% nonfat dry milk dissolved in Tris-buffered saline with Tween-20 (TBST) at room temperature for 1 h. The membranes were combined with primary antibodies overnight in a 4°C freezer. On the following day, the membranes were washed three times, and then incubated with secondary antibodies.

Real-time quantitative PCR

Real-time quantitative PCR (qRT-PCR) was performed to determine the relative expression of circRNA: circ-HECTD1 and *Hectd1* mRNAs. Total RNA was extracted from HPF-a cells with TRIzol reagent (Invitrogen) according to the manufacturer's instructions. After the extraction of total RNA, the concentration of RNA was measured by NanoDrop One (Thermo Fisher Scientific). The various samples were normalized to contain 300 ng or 400 ng of RNA and reverse-transcribed into cDNA; the cDNA samples were used as templates for real-time qRT-PCR. Cycle threshold (Ct) and ΔCT values were analyzed. The ΔΔCT quantification method was performed using Opticon Monitor software (Bio-Rad). The relative quantitative expression of RNA was normalized to that of the endogenous reference (GAPDH).[29]

CRISPR/Cas9 plasmid transfection technology

CRISPR/Cas9 double nickase plasmids (HECTD1-NIC) were used to knock down HECTD1, which was purchased from Santa Cruz Biotechnology®. According to the manufacturer's protocol, approximately 1×10^5 cells were seeded into every well at first using pure DMEM. The cells were grown until 50–80% confluency. At the start of the transfection experiment, 0.1 μg of plasmid was added to the transfection medium, and 0.5 μl of UltraCruz® Transfection Reagent was added to the transfection medium. Then, 10 μl of each plasmid was added to each well. The cells were kept quiescent for 5 min, then the two solutions were mixed and immediately vortexed at room temperature and incubated for ⩾20 min. Solutions were added into wells, and after waiting for at least 12 h, the standard medium was replaced. The samples were incubated for 24–72 h in an incubator at 37°C until use for subsequent experiments.[10]

Immunofluorescence staining

After experimental treatment of the cells seeded in 24-well plates on coverslips, the cells were washed twice with cold PBS to remove the remaining medium and fixed in 4% paraformaldehyde at 4°C overnight. The following day, the coverslips were blocked with 10% normal goat serum in 0.3% Triton X-100 for 2 h at room temperature and incubated with primary antibodies (HECTD1 or vimentin) at 4°C overnight. The next day, the cells were incubated with the appropriate fluorescent secondary antibodies (Alexa Fluor, Thermo Fisher Scientific), and the nuclei were stained with 4′,6-diamidino-2-phenylindole (DAPI). A fluorescence microscope (Olympus IX70, Olympus America, Inc., Center Valley, PA, USA) was used to capture images of the cells.

2D scratch and 3D nested matrix model cell migration assay

A 2D scratch assay and 3D migration assay were performed to measure cell migration capacity.

Specifically, we seeded HPF-a GFP cells in 24-well plates at a density of 1×10^5 cells in every well and continued to culture in a 37°C incubator until they were close to fill in wells. Then, we used a sterile 200-μl pipette tip to scratch a straight line of moderate width. Similarly, we scratched a new straight line perpendicular to the first line to create a cross-shaped cellular gap in each well. The medium was removed, and wells were washed twice with PBS to wash out the cell debris, and fresh standard medium was then added to each well to ensure cell growth. Simultaneously, cells were treated with 50 μg/cm^2 SiO_2, and digital images of the scratch gap were captured immediately and then subsequently at 12, 24, and 48 h. ImageJ software was used to measure the distance of the cell gaps. Each experiment was repeated at least three times.[8]

Fluorescent in situ hybridization

Fluorescent in situ hybridization (FISH) was used to detect circHECTD1 expression in HPF-a cells. First, we seeded HPF-a cells on sterile coverslips at a density of 1×10^4 in 24-well plates. After experimental treatment, the coverslips were washed twice with DEPC PBS, and then blocked for 20 min at room temperature with 4% PFA. Cells were washed twice with DEPC PBS, permeabilized with 0.25% Triton X-100 for 15 min, and subjected to two 15-min washes with saline sodium citrate (SSC) buffer and prehybridized in hybridization solution for 1 h at 37°C. The cells were then incubated with the labeled probe (circHECTD1) in hybridization solution at 37°C overnight. The following day, the coverslips were washed and incubated in blocking buffer for 1 h at room temperature. The samples were then incubated with FITC at 4°C overnight. The next day, the cells were washed with DEPC PBS and mounted with DAPI. A fluorescence microscope was used to capture the cell images.

Bromodeoxyuridine labeling

Cells were prepared on poly-L-lysine (PLL)-coated coverslips. Bromodeoxyuridine (BrdU) (Yeasen, 40204ES60) reagent was dissolved in PBS, added to the medium (1:1000) and incubated 6 h before fixation. The cells were fixed in 4% PFA at 4°C overnight, washed twice with PBS, denatured in 2 *N* HCl at room temperature for 30 min and then rinsed in 0.1 M borate buffer (pH 8.0, 200 μl/well) for 10 min. After incubation in blocking solution (PBS containing 10% NGS and 0.3% Triton X-100) for 1 h, cells were treated with mouse anti-BrdU antibody (1:200; SC-32323, Santa Cruz) overnight at 4°C. After a wash stage with PBS, cells were incubated with donkey anti-mouse (conjugated to Alexa Fluor 576) secondary antibodies for 2 h at room temperature. They were then washed three times in PBS and mounted using mounting solution (Prolong Gold anti-fade reagent with DAPI; P36931, Life Technologies). Association slides were imaged using a fluorescence microscope (Olympus IX70, Olympus America, Inc., Center Valley, PA, USA). Five fields per well were randomly selected for cell counting.

Hoechst 33342 staining

HPF-a grown on poly-L-lysine-coated glass cover slips were stained using Hoechst 33342 (10 μg/ml) after treatment with BD1047 for 2 h and SiO_2 for 24 h. Briefly, HPF-a were stained with Hoechst 33342 for 5 min at room temperature and then fixed in 4% paraformaldehyde (PFA) for 20 min. The population of apoptotic cells was observed under a fluorescence microscope. Five fields per well were randomly selected for apoptosis cell counting.[16]

(4,5-Dimethylthiazol-2-yl)-2,5-diphenyltetrazolium bromide (MTT) assay

Cell viability was measured using MTT assays as previously described.[8]

Lentiviral transfection

P2-5 generations of HPF-a cells were transfected with circHECTD1 lentivirus (HANBIO Inc., Shanghai, China) as previously described.[8]

Statistics

The data are presented as the mean ± standard error of the mean (SEM). Statistical analyses were performed using the Student's *t* test or two-way analysis of variance (ANOVA) with SigmaPlot 11.0. The tests used are indicated in the figure legends. The ANOVA results were considered significant at a $p < 0.05$.

Results

HECTD1 expression was induced in HPF-a cells after exposure to silica and increased in fibroblasts derived from patients with silicosis

Our laboratory's previous reports have indicated that HECTD1 plays an important role in macrophage activation[10]; however, little is known about the effect of HECTD1 in fibroblast activation and the progression of silicosis. According to previous dosage experiments, we set the concentration at 50 μg/cm^2 for all related experiments.[7,30] To identify whether HECTD1 is involved in silicosis, the HPF-a cell line was exposed to SiO_2 and assessed for HECTD1 expression. Immunoblotting results in Figure 1(a,b) show that HECTD1 expression increased at 1, 3, 6, and 12 h, and peaked at 6 h after SiO_2 treatment. This finding was further confirmed by immunostaining of the HECTD1 protein in HPF-a cells (Figure 1c). In the silicosis mouse model, immunohistochemistry revealed an increase in fibroblasts in the lungs, as indicated by an increase in vimentin, a specific fibroblast marker, which suggested aggravation of the fibrosis process. Additionally, HECTD1 expression was upregulated in mouse lungs after SiO_2 exposure and colocalized with the fibroblast marker vimentin (Figure 1d). Furthermore, compared with lung tissues from healthy donors, the immunohistochemistry staining of patients with late stage silicosis showed that vimentin and HECTD1 increased (Figure 1e), which confirmed previous findings in HPF-a cells.

HECTD1 regulates fibroblast proliferation and activation in HPF-a

Pulmonary fibrosis is due mainly to the activation of fibroblasts, which are characterized by excessive proliferation and migration;[7,31] therefore, we first investigated the role of HECTD1 in HPF-a activation in response to SiO_2 exposure. Previous studies have indicated that SiO_2 causes HPF-a viability to increase in a time-dependent manner. CRISPR/Cas9 technology (Figure S1) was applied to knock down the HECTD1 protein (HECTD1-NIC), increasing the fibroblast activation markers, collagen 1 and α-SMA (Figure S2a). Moreover, HECTD1-NIC treatment also abolished the increased cell viability induced by SiO_2 (Figure 2a), as confirmed by the gel contraction assay, which has been widely adopted in the assessment of fibroblast activation (Figure 2b,c). To test the proliferation of HPF-a cells, the BrdU assay was performed. The number of newborn cells increased upon SiO_2 treatment, while the number of BrdU-positive cells decreased sharply after HECTD1-NIC treatment (Figure 2d,e). After confirming the role of HECTD1 in the increase in cell proliferation, whether HECTD1 is also involved in the decrease in apoptosis induced by SiO_2 was also investigated. As shown in Figure 2(f,g), SiO_2 induced a decrease in the ratio of BAX/Bcl-XL, indicating a decrease in cell apoptosis, and this effect was reversed by HECTD1-NIC. Moreover, HECTD1-NIC induced apoptosis in the control, as indicated by increases in the BAX/Bcl-xL levels (Figure 2f,g). The role of HECTD1 in cell apoptosis induced by SiO_2 was confirmed by the Hoechst assay (Figure 2h,i).

HECTD1 mediates silica-induced cell migration in HPF-a

Considerable evidence has suggested that pulmonary fibroblast migration is one main causes of pulmonary fibrosis,[32–34] and we thus explored the role of HECTD1 in SiO_2-mediated cell migration. The results of the scratch assay in Figure 3(a,b) show that SiO_2 promoted the migration of HPF-a cells, which was significantly inhibited by HECTD1-NIC. Moreover, overexpression of HECTD1 enhanced HPF-a cell migration (Figure S2b), confirming the role of HECTD1 in cell migration. To validate the cell migration ability, the 3D nested matrix cell migration model was applied, which is better for simulating the *in vivo* environment. As shown in Figure 3c–(e), HECTD1-NIC not only inhibited the number of migrated cells but also limited the maximum migrated distance of HPF-a cells induced by SiO_2, similar to the result of the 2D scratch assay. Furthermore, we measured the expression of the migration marker and found that the increase in p-PYK2 was induced by SiO_2 (Figure 3f,g). Moreover, knocking down the HECTD1 reversed the upregulation of p-PYK2 induced by SiO_2 (Figure 3h,i).

HECTD1 mediates autophagic processes in fibroblasts exposed to silica

Next, we wanted to investigate the molecular mechanism of HECTD1 in fibroblast activation induced by SiO_2. An increasing number of reports have indicated that autophagy plays an important

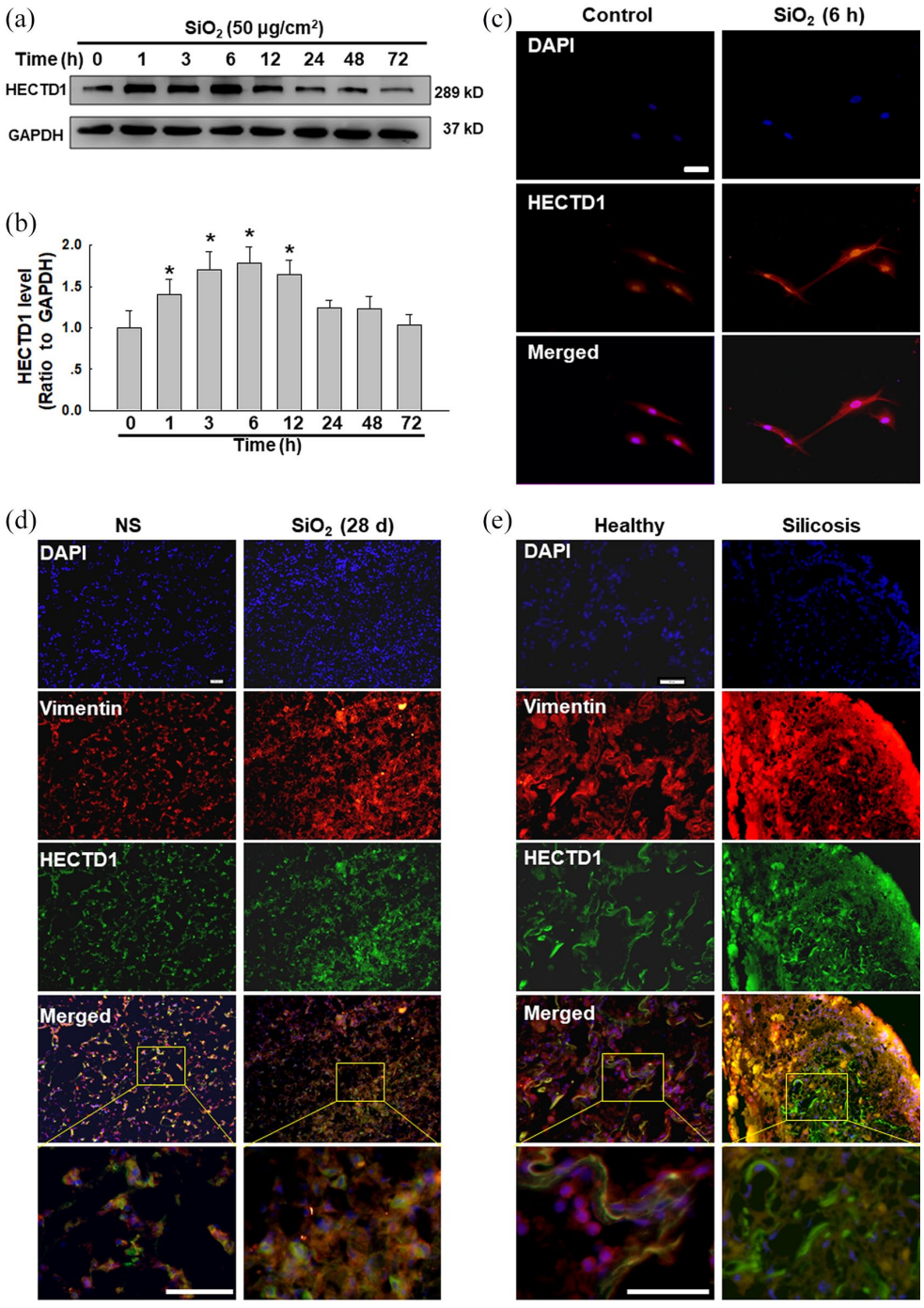

Figure 1. HECTD1 expression was induced in HPF-a cells after exposure to silica and increased in fibroblasts derived from patients with silicosis.
(a) Representative western blot showing SiO_2-induced HECTD1 upregulation in a time-dependent manner. (b) Densitometric analysis of HECTD1 from five experiments; *$p < 0.05$ *versus* the control group; $n = 5$. (c) Representative images of immunocytochemical staining showing that SiO_2 (50 mg/cm^2) increased the HECTD1 protein in HPF-a cells 6 h after the initiation of SiO_2 treatment. Scale bar = 50 μm. (d) Immunohistochemistry of the fibroblast marker vimentin and HECTD1 protein in the lung tissues of mice exposed to NS or SiO_2. Colocalization of vimentin and HECTD1 protein is shown. The images are representative of several individuals from each group. Scale bar = 20 μm. (e) Representative images of immunohistochemical staining show the expression of vimentin and HECTD1 in lung sections from healthy donors and patients with silicosis. Scale bar = 20 μm.
HECTD1, domain-containing E3 ubiquitin protein ligase 1; NS, normal saline; SiO_2, silicon dioxide.

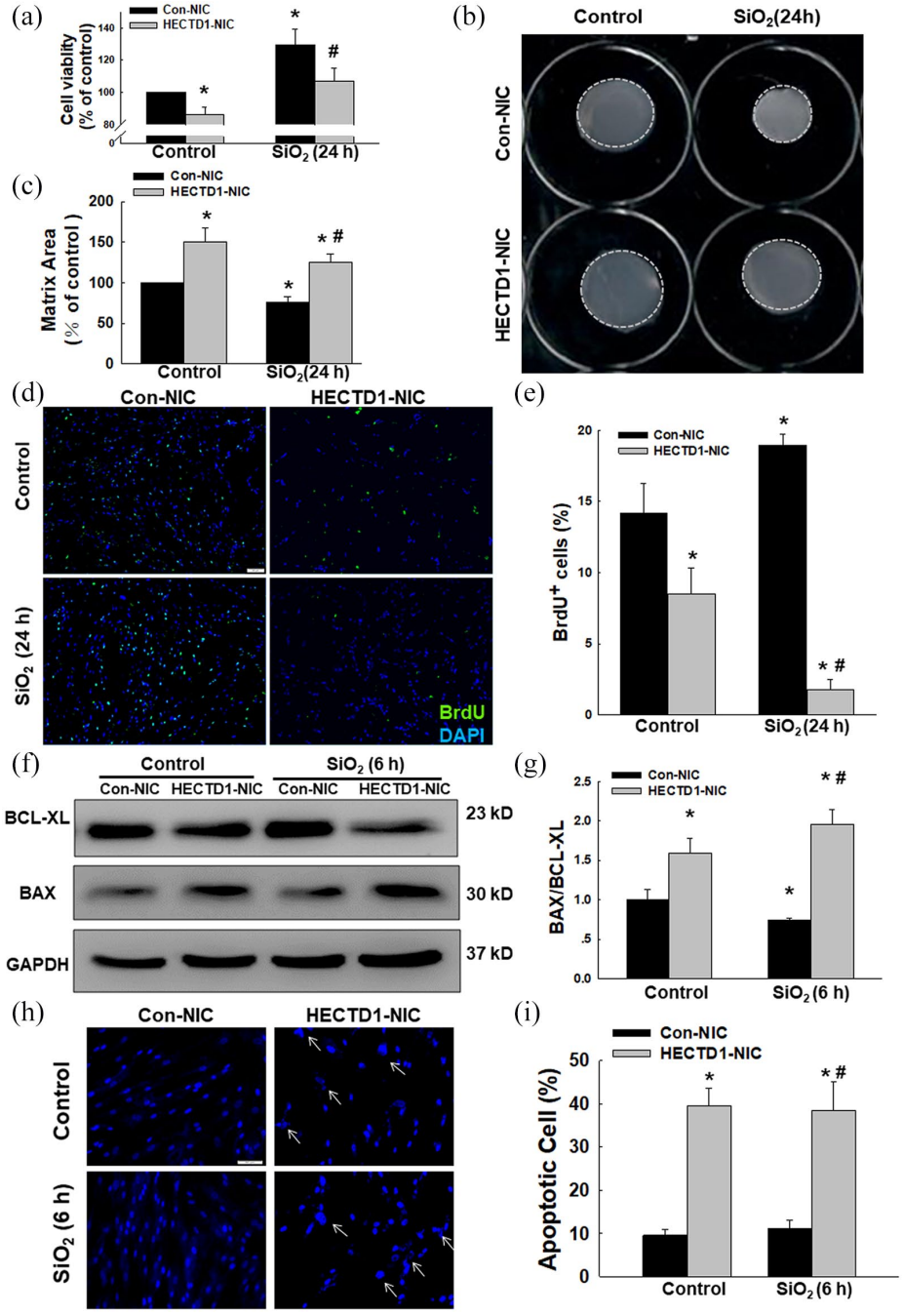

Figure 2. HECTD1 regulates fibroblast proliferation and activation in HPF-a cells.
(a) MTT assay showing that the SiO_2-induced increase in cell viability was reversed by HECTD1 knockdown; $^{*}p < 0.05$ *versus* the corresponding control group; $^{\#}p < 0.05$ *versus* the SiO_2 group; $n = 5$. (b) Representative images of collagen gel sizes showing the effects of SiO_2 on gel contraction (indicating fibroblast activation). (c) Quantification of the matrix area in five separate experiments. $^{*}p < 0.05$ *versus* the corresponding control group; $^{\#}p < 0.05$ *versus* the SiO_2 group. (d) Immunofluorescence for BrdU (green) and DAPI (blue). Merged image demonstrating that proliferation induced by SiO_2 was attenuated by HECTD1 knockdown. Scale bar = 50 μm. (e) Percent of BrdU-positive cells from five separate experiments. $^{*}p < 0.05$ *versus* the corresponding control group; $^{\#}p < 0.05$ *versus* the SiO_2 group. (f) Representative western blot showing the effects of HECTD1-NIC transfection on SiO_2-induced BAX and BCL-XL expression in HPF-a cells. (g) Densitometric analyses of five separate experiments suggested that BAX expression was enhanced by HECTD1-NIC transfection, but BCL-XL expression was decreased. $^{*}p < 0.05$ *versus* the corresponding control group; $^{\#}p < 0.05$ *versus* the SiO_2 group. (h) Representative images of Hoechst 33342 staining depicting apoptosis of HPF-a cells was enhanced by HECTD1-NIC. Scale bar = 50 μm. (i) Percentages of apoptotic cells from five independent experiments are presented. $^{*}p < 0.05$ *versus* the control group. $^{\#}p < 0.05$ *versus* the SiO_2 group.

(Continued)

Figure 2. (Continued)

BrdU, bromodeoxyuridine; DAPI, 4′,6-diamidino-2-phenylindole; HECTD1, domain-containing E3 ubiquitin protein ligase 1; MTT, (4,5-dimethylthiazol-2-yl)-2,5-diphenyltetrazolium bromide; NS, normal saline; SiO_2, silicon dioxide.

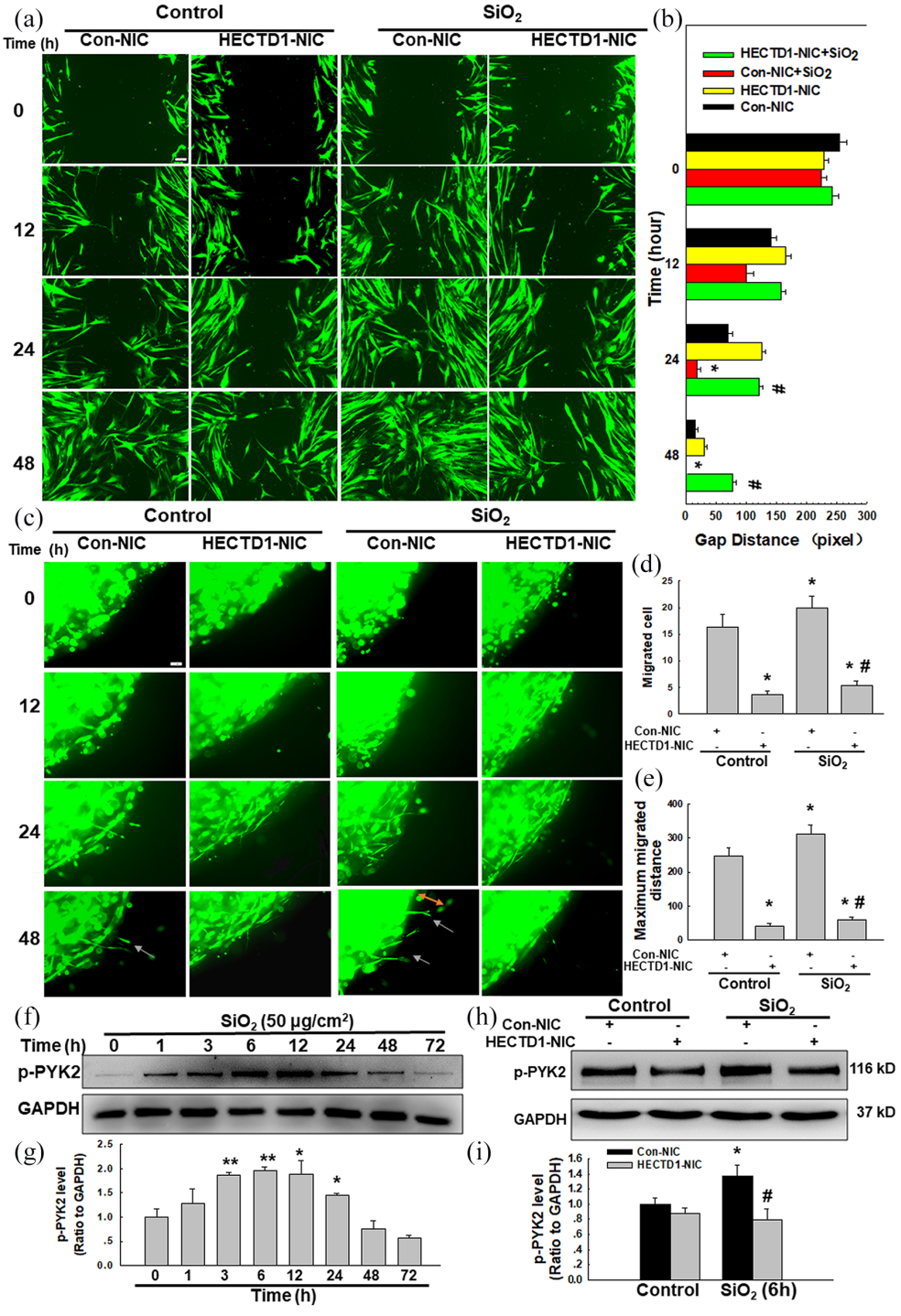

Figure 3. HECTD1 mediates silica-induced cell migration in HPF-a cells.
(a) Representative images showing the SiO_2-induced increase in cell migration using a scratch assay was attenuated by HECTD1-NIC. Scale bar = 50 μm. (b) Quantification of the scratch gap distances from five independent experiments; *$p < 0.05$ *versus* the corresponding time point in the control group; #$p < 0.05$ *versus* the corresponding time point in the

(Continued)

Figure 3. (Continued)

SiO_2 group. (c) Representative images of SiO_2-induced cell migration in a nested gel matrix; this migration was abolished by HECTD1-NIC. Scale bar = 50 μm. Quantification of the number of migrated cells (white arrows) from the nested gel matrix (d) and the maximum migrated distance (red arrows) (e) from five separate experiments. $^*p < 0.05$ *versus* the corresponding time point in the control group; $^\#p < 0.05$ *versus* the corresponding time point in the SiO_2 group. (f,h) Representative western blot showing that SiO_2-induced phosphorylation of PYK2 occurred in a time-dependent manner and was attenuated by HECTD1-NIC. (g,i) Densitometric analysis of the phosphorylation of PYK2 expression from five experiments; $^*p < 0.05$ *versus* the control group; $^\#p < 0.05$ *versus* the corresponding time point in the SiO_2 group.
HECTD1, domain-containing E3 ubiquitin protein ligase 1; SiO_2, silicon dioxide.

role in animal models of silicosis.[35,36] In our previous study, we confirmed that autophagy in macrophages is involved in SiO_2-induced fibrosis.[16] Whether autophagy is also critical in fibroblasts in response to silica, and how it affects the development of silicosis remains unknown. We first examined the protein expression of ATG5, BECN, and LC3B, which are markers of autophagy. Notably, western blot results showed significantly increased expression of autophagy markers following silica exposure, which peaked at 6 h (Figure 4a,b). As shown in Figure 4(c,d), knocking down HECTD1 reduced the expression of ATG5, BECN, and LC3B. To further validate this result, HPF-a cells were transduced with dual fluorescent–mRFP–GFP-MAP1LC3-adenovirus. The latter was used to detect the cell autophagy process, which was applied to monitor autophagosome formation in real time by fluorescence microscopy. mRFP was used to label and track LC3, whereas GFP fluorescence is sensitive to acidic conditions such that GFP fluorescence will be quenched when a lysosome and an autophagosome form an autolysosome.[37] As a consequence, the colocalization of GFP and RFP signals (yellow dots) represents autophagosomes that have not fused with lysosomes; only red fluorescence was detected under the microscope when autophagic flux was induced. As shown in Figure 4(e),f, SiO_2 significantly induced autophagic flux, and this effect of SiO_2 was attenuated by knocking down HECTD1. Moreover, HECTD1-NIC also attenuated cell autophagy in normal cells without SiO_2 exposure, confirming the role of HECTD1 in autophagy (Figure S3a).

HECTD1-mediated autophagy regulates the activation and migration of HPF-a cells

As an increasing number of studies have suggested that autophagy is associated with cell activation and migration in silicosis,[37] we hypothesized that HECTD1 mediates fibroblast activation and migration *via* autophagy. To test this hypothesis, rapamycin, a specific activator of autophagy, was applied. As shown in Figure 5(a,b), pretreatment with rapamycin (5 μg/μl) reversed the decrease in cell migration caused by HECTD1 NIC. It is suggested that HECTD1 induced fibroblast activation *via* autophagy. Similarly, rapamycin reversed the effect of HECTD1-NIC in both cases in the SiO_2 group (Figure S3b). Moreover, pretreatment with rapamycin eliminated the attenuated effects of fibroblast viability caused by HECTD1-NIC (Figure 5c). Since HECTD1-NIC inhibited the increase in cell viability induced by SiO_2, rapamycin attenuated the effect of HECTD1-NIC on SiO_2, indicating the upstream effector of autophagy was HECTD1. To further confirm the role of autophagy and HECTD1 in cell vitality, the specific autophagy inhibitor bafilomycin A1 was applied. As shown in Figure S4 bafilomycin A1 further decreased cell migration in the HECTD1-NIC group, indicating the effect of autophagy and HECTD1 on cell migration and viability.

Expression of circHECTD1 in fibroblasts after SiO_2 treatment

Having confirmed the crucial role of HECTD1 in fibroblast function in response to silica, we next aimed to understand the molecular mechanism related to HECTD1 regulation. Interestingly, the mRNA expression of *Hectd1* did not show any change after SiO_2 exposure (Figure 6a), indicating that posttranscriptional mechanisms may be involved in the regulation of HECTD1. Recently, there has been increasing evidence indicating that circRNAs are linked to a variety of diseases,[17,20,21] but little research has been conducted regarding the roles of circRNAs in the development of silicosis. We established a mouse model of silicosis, and then performed high-throughput screening. We analyzed 120 circRNAs that were differentially expressed in the SiO_2 group compared with the control group.[10] One of them, hsa_circ_0101590 (mm9_circ_002888, circHECTD1), caught our

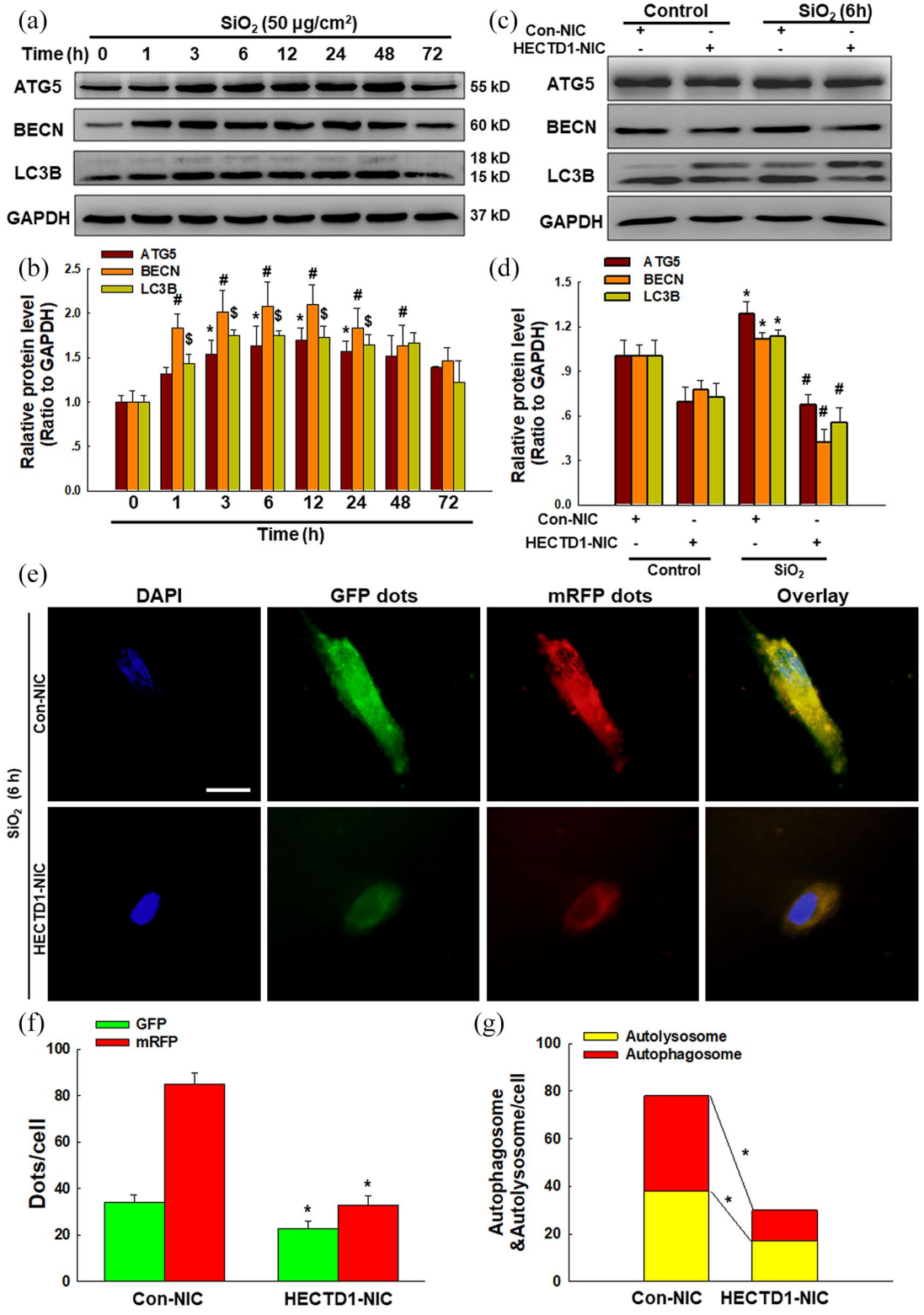

Figure 4. HECTD1 mediates autophagic processes in fibroblasts exposed to silica.
(a) Representative western blot showing the effects of SiO_2 on the expression of the autophagy markers ATG5, BECN and LC3B in HPF-a cells. (b) Densitometric analyses of five separate experiments suggested that SiO_2 induced increases in ATG5, BECN and LC3B expression. $^{*}p < 0.05$ *versus* ATG5 expression at 0 h; $^{\#}p < 0.05$ *versus* BECN expression at 0 h; $^{\$}p < 0.05$

(Continued)

Figure 4. (Continued)

versus LC3B expression at 0 h; (c) Representative western blot showing the effects of HECTD1 knockdown on the SiO_2-induced expression of ATG5, BECN and LC3B in HPF-a cells at 6 h following 50 μg/cm^2 SiO_2 treatment. (d) Densitometric analyses of five separate experiments suggested that HECTD1-NIC attenuated the SiO_2-induced increases in ATG5, BECN and LC3B expression. *$p < 0.05$ *versus* the control group; #$p < 0.05$ *versus* the corresponding SiO_2 group. (e) Representative images showing the effects of HECTD1-NIC on the SiO_2-induced formation of RFP- and GFP-MAP1LC3 puncta at 6 h following SiO_2 treatment. Scale bar = 10 μm. Red arrows indicate autolysosomes; yellow arrows indicate autophagosomes. (f) Quantification of the RFP- and GFP- MAP1LC3 puncta demonstrating that SiO_2-induced autophagy was attenuated by HECTD1 NIC. *$p < 0.05$ *versus* the Con-NIC group; (g) Quantification of RFP-MAP1LC3 puncta and RFP- and GFP-colocalized puncta demonstrating autophagic flux induced by SiO_2 was attenuated by HECTD1-NIC. *$p < 0.05$ *versus* the Con-NIC group. HECTD1, domain-containing E3 ubiquitin protein ligase 1; SiO_2, silicon dioxide.

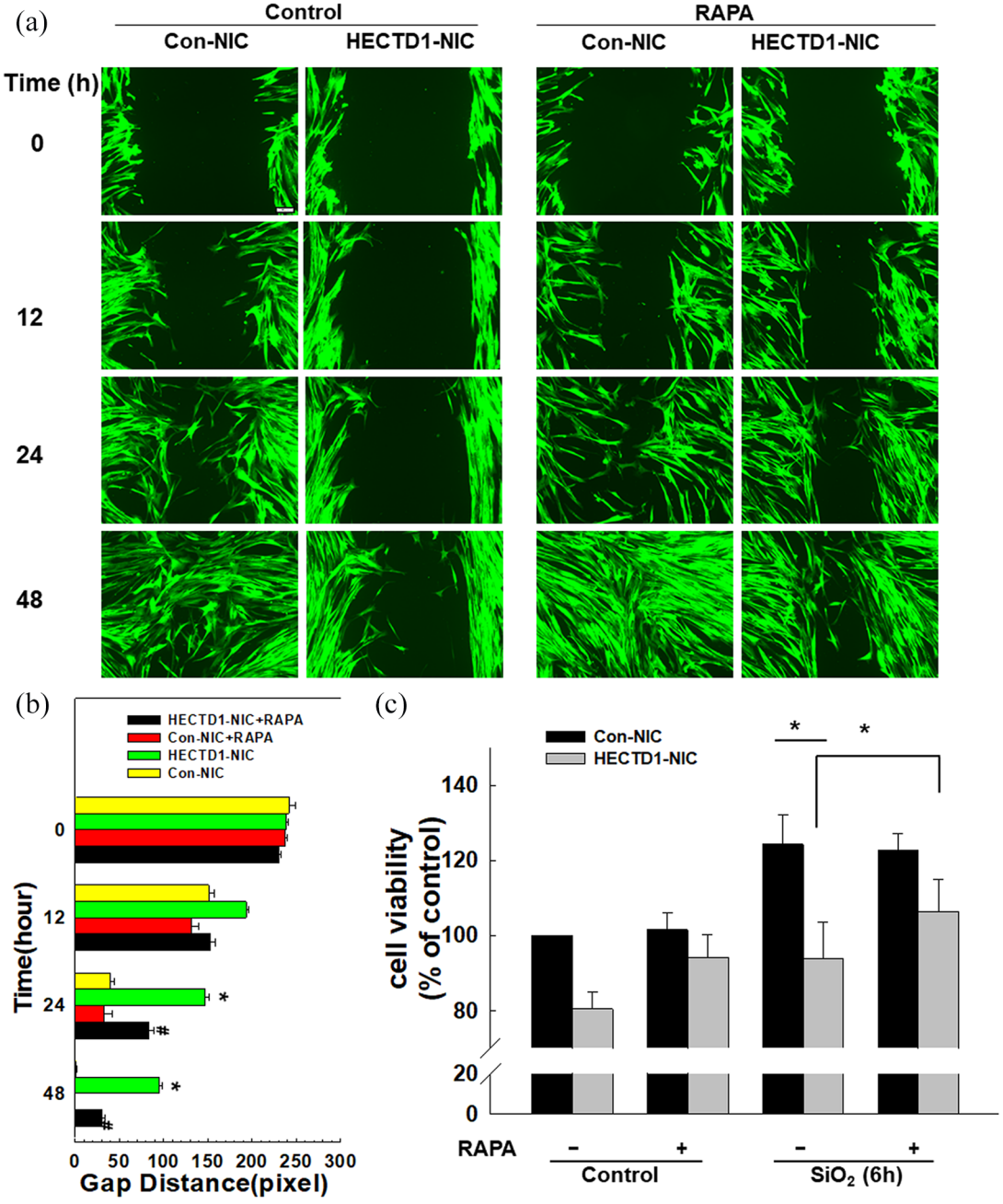

Figure 5. *(Continued)*

Figure 5. HECTD1-mediated autophagy regulates activation and migration in HPF-a cells.
(a) Representative images showing that HECTD1 knockdown inhibited cell migration, which was reversed by pretreatment with rapamycin (5 μg/μl). Scale bar = 50 μm. (b) Quantification of the scratch gap distance from five separate experiments. *$p < 0.05$ *versus* the Con-NIC group at the corresponding time points. #$p < 0.05$ *versus* the HECTD1-NIC group at the corresponding time points. (c) MTT assay showing that HECTD1 knockdown inhibited cell viability and was reversed by pretreatment with rapamycin. *$p < 0.05$ *versus* the corresponding control group; $n = 5$.
HECTD1, domain-containing E3 ubiquitin protein ligase 1; MTT, (4,5-dimethylthiazol-2-yl)-2,5-diphenyltetrazolium bromide; SiO_2, silicon dioxide.

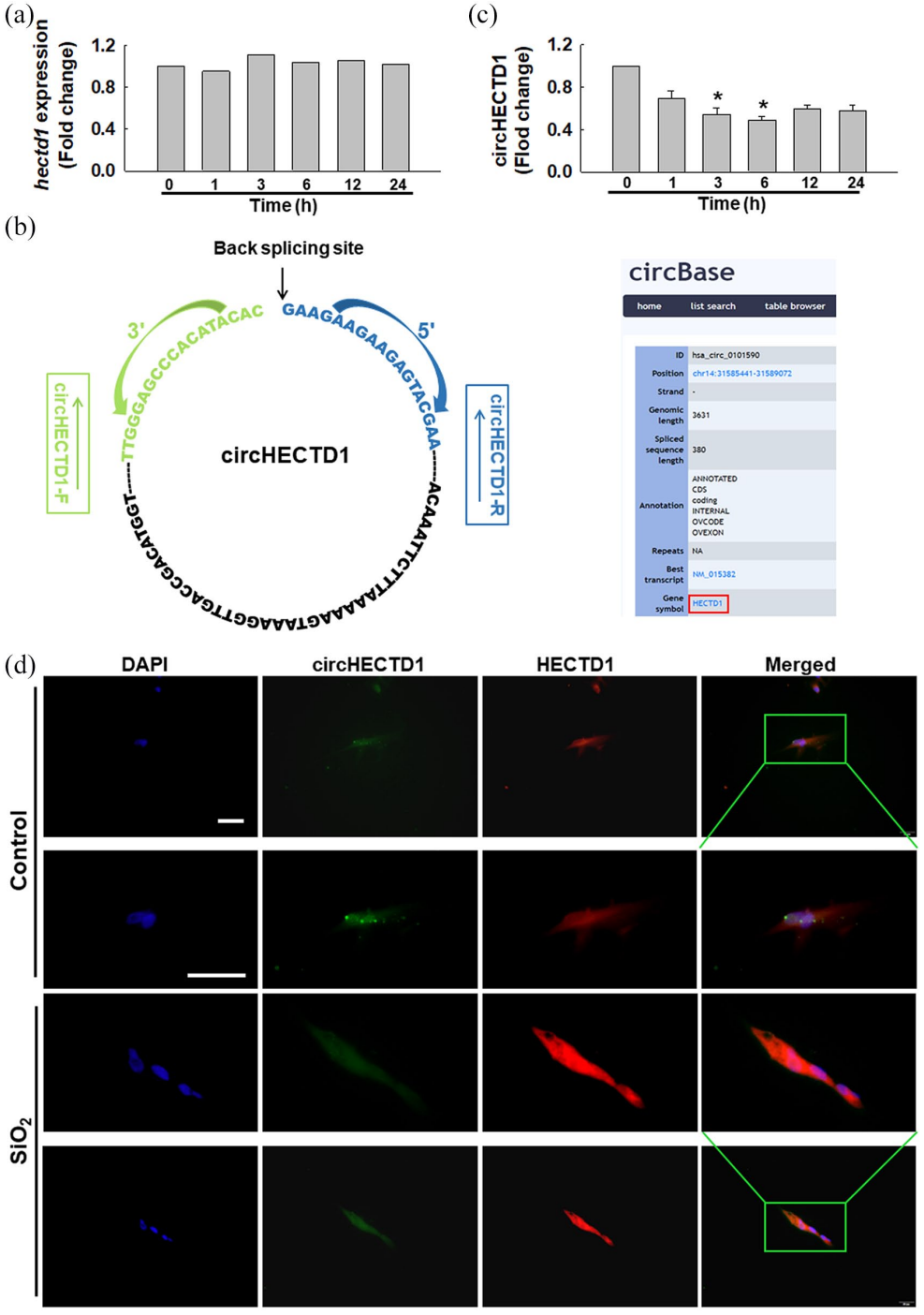

Figure 6. *(Continued)*

Figure 6. Expression of circHECTD1 in fibroblasts after SiO_2 treatment.
(a) qRT-PCR analysis showing the expression of HECTD1 mRNA did not change after HPF-a cells were exposed to SiO_2; $^*p < 0.05$ *versus* 0 h; $n = 5$. (b) Structures and probe sequence of circHECTD1, as well as ID number and alias of hsa_circ_0101590 from the circBase database. (c) As shown in the qRT-PCR analysis, circHECTD1 expression in HPF-a cells was decreased after exposure to SiO_2; $^*p < 0.05$ *versus* circHECTD1 expression at 0 h; $n = 5$. (d) FISH assay showing circHECTD1 expression in HPF-a cells exposed to SiO_2. circHECTD1 was labeled with fluorescein isothiocyanate, and immunocytochemical staining showed that SiO_2 increased the HECTD1 protein expression in HPF-a cells. Scale bar = 20 μm.
HECTD1, domain-containing E3 ubiquitin protein ligase 1; FISH, fluorescence in situ hybridization; qRT-PCR, quantitative real-time PCR; SiO_2, silicon dioxide.

attention because its host gene is *Hectd1* (Figure 6b). Thus, we tested the expression levels of circHECTD1 in HPF-a cells by qRT-PCR. circHECTD1 RNA expression was downregulated within 24 h after SiO_2 treatment (Figure 6c). These results were confirmed by a FISH assay, in which circHECTD1 was detected mainly in the cytoplasm of HPF-a cells (Figure 6d). Furthermore, SiO_2 induced a rapid decrease in circHECTD1 expression *in vitro* and increased the protein expression of HECTD1 (Figure 6d).

circHECTD1 is involved in SiO_2-induced HECTD1 upregulation and affects the function of cells

To further understand the interaction between circHECTD1 and HECTD1, specific overexpression was applied using a circHECTD1 lentivirus (Figure 7a). As shown in Figure 7(b,c), circHECTD1 overexpression not only decreased the level of the HECTD1 protein in normal HPF-a cells but also inhibited the HECTD1 level in HPF-a cells exposed to SiO_2, while circHECTD1 overexpression had no effect on *Hectd1* mRNA expression (Figure 7d). Moreover, specific knockdown of circHECTD1 *via* siRNA upregulated the expression of HECTD1, indicating the regulatory effect of circHECTD1 on HECTD1 (Figure S5). Next, to clarify whether circHECTD1 was involved in SiO_2-induced fibroblast activation and migration, circHECTD1 overexpression was applied in the cell migration and viability assays. The SiO_2-induced increases in HPF-a cell migration (Figure 7e,f) and viability (Figure 7g) were also significantly reversed after circHECTD1 overexpression.

Discussion

Numerous studies have shown that pulmonary fibrosis is mainly caused by the activation of macrophages, which release inflammatory factors and cytokines to influence the activation and migration of downstream effector cells.[1,4,5,31] However, the direct effects of SiO_2 on protein production and functional changes in pulmonary fibroblasts have not been studied extensively. The current study focused mainly on functional changes in fibroblasts in the fibrosis stage, which suggests that the direct effect of SiO_2 on fibroblasts may play an important role in the pathogenesis of silicosis (Figure 8).

Previous data suggest that fibroblast activation and migration are the main properties of silicosis. However, the detailed mechanism involved in this process remains unclear. Our group previously demonstrated that HECTD1 participates in the regulation of pulmonary fibrosis through ubiquitination,[10] and plays an important role in endothelial-to-mesenchymal transition (EndoMT),[38] indicating that HECTD1 might be involved in functional cellular changes in silicosis. HECTD1, which encodes a novel protein homologous to the E6-AP C-terminal (HECT) domain-containing E3 ubiquitin (Ub) ligase, plays an important role in the ubiquitin-proteasome system.[10] Moreover, HECTD1 plays a vital role in regulating cell migration *via* PIPKIγ90.[39] It is also involved in neural tube defects and abnormalities in the cranial mesenchyme *via* Hsp90,[40] and HECTD1 expression is upregulated in fibroblasts obtained from primary sites, lymph nodes, and bone marrow of patients with breast cancer.[41] Currently, HECTD1 is suggested to promote cell proliferation and migration *via* autophagy in fibroblasts after exposure to silica. Interestingly, HECTD1 induced cell apoptosis in macrophages and endothelia cells exposure to silica,[10,42] which is in contrast to the role of HECTD1 in fibroblasts. Ubiquitination mediated by E3 ligase-HECTD1 has paradoxical effects, and may exhibit different functions that depends on its target proteins, such as autophagy-related proteins. Moreover, silica induced different expression patterns in macrophages, endothelial cells, and fibroblasts, indicating the complex role of HECTD1 in inflammation and fibrosis. Thus, the detailed

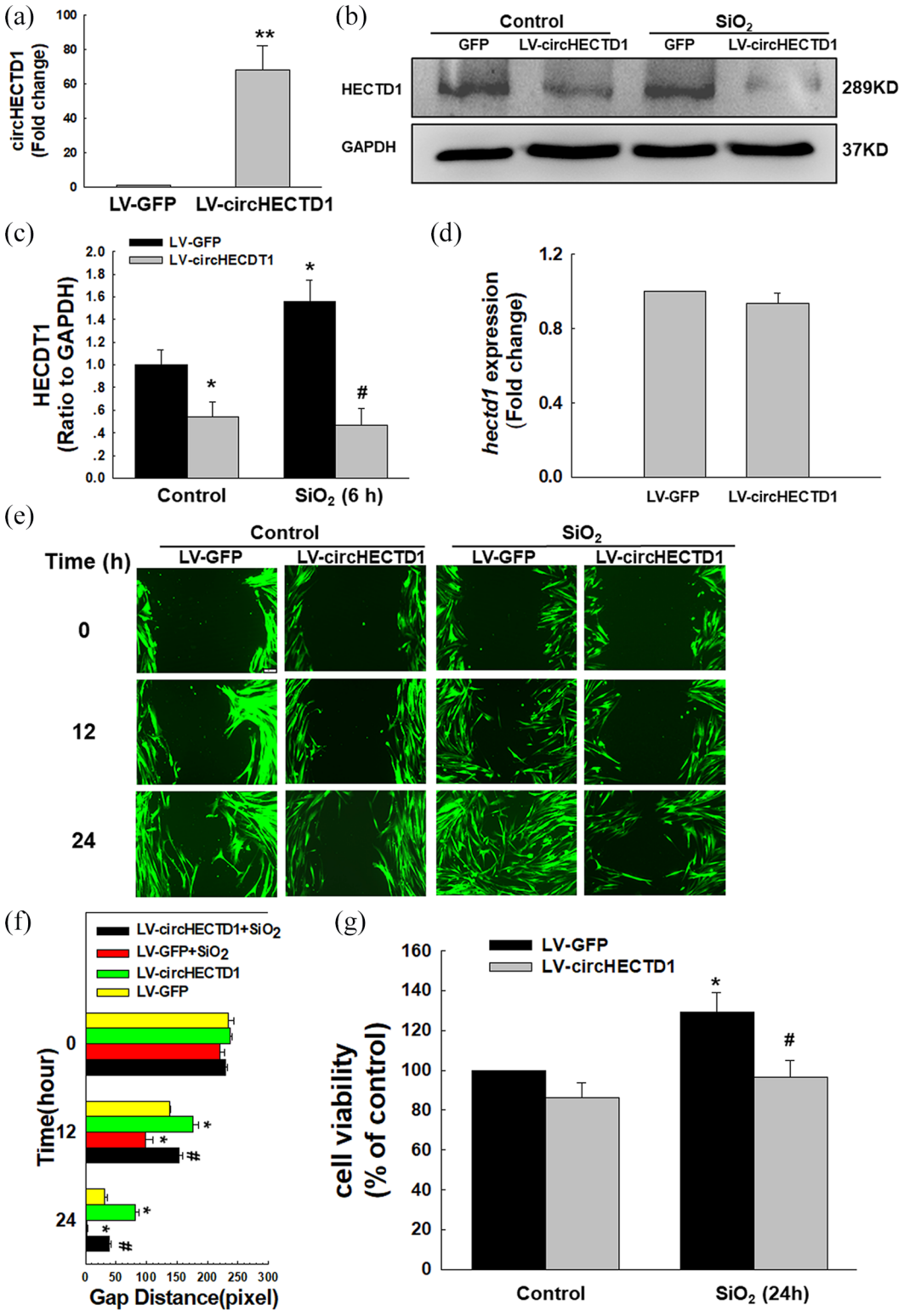

Figure 7. circHECTD1 is involved in SiO_2-induced HECTD1 upregulation and affects the function of cells.
(a) As shown in the qRT-PCR analysis, transfection of the circHECTD1 lentivirus upregulated circHECTD1 expression in HPF-a cells. $^{**}p < 0.01$; $n = 5$. (b) Representative western blot showing the effect of specific overexpression of circHECTD1 with lentivirus on SiO_2-induced HECTD1 expression. (c) Densitometric analyses of five separate experiments suggested

(Continued)

Figure 7. (Continued)

that SiO_2-induced changes in HECTD1 expression are attenuated by circHECTD1 upregulation. *$p < 0.05$ *versus* the levels of the corresponding protein in the control group; #$P<0.05$ vs. the levels of the corresponding protein in the SiO_2 group. (d) qRT-PCR analysis showing that the expression of the *Hectd1* mRNA did not change in HPF-a cells after overexpression of circHECTD1; $n = 5$. (e) Representative images showing that the effect of SiO_2 on GFP-labeled HPF-a cell migration in scratch assays was attenuated by circHECTD1 overexpression. Scale bar = 50 μm. (f) Quantification of the scratch gap distances in five separate experiments. *$p < 0.05$ *versus* the control group; #$p < 0.05$ *versus* the SiO_2 group. (g) MTT assay showing that the SiO_2-induced increase in cell viability was reversed by circHECTD1 overexpression; *$p < 0.05$ *versus* the control group; #$p < 0.05$ *versus* the SiO_2 group; $n = 5$.
HECTD1, domain-containing E3 ubiquitin protein ligase 1; MTT, (4,5-dimethylthiazol-2-yl)-2,5-diphenyltetrazolium bromide; qRT-PCR, quantitative real-time PCR; SiO_2, silicon dioxide.

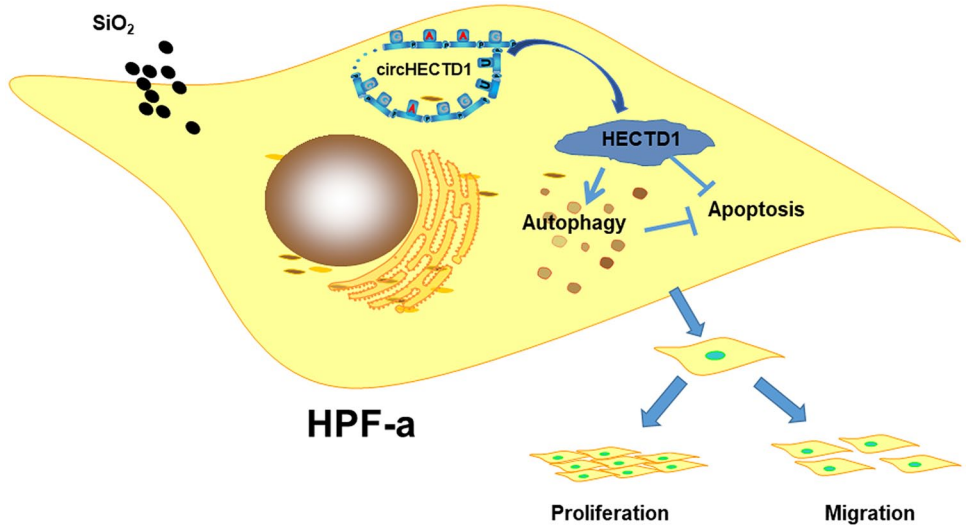

Figure 8. Schematic diagram showing the mechanisms by which circHECTD1/HECTD1 mediates SiO_2-induced pulmonary fibrosis.
HECTD1, domain-containing E3 ubiquitin protein ligase 1; SiO_2, silicon dioxide.

regulatory mechanism of HECTD1 in silicosis deserves further investigation.

circRNAs are a new class of noncoding RNAs that are very stable due to their special cyclic structures. Cumulative evidence has revealed that circRNAs are related to disease processes, and act as important biomarkers of various diseases. circRNAs can act as gene expression regulators *via* different regulatory modes.[10] For example, they are involved in the regulation of transcription and alternative splicing,[43] and can interact with ribonucleoproteins (RBPs),[44] acting as a miRNA sponge,[45,46] or even be translated into proteins.[47] Recent studies have suggested that a posttranscriptional mechanism was associated with circHECTD1 in HECTD1 regulation and silicosis. According to our previous silicosis mouse circRNA microarray data and pulmonary fibrosis studies, we selected circHECTD1 as our target.[10] In this study, we confirmed that circHECTD1 expression is downregulated in HPF-a cells after silica exposure. In addition, we found that overexpressed circHECTD1 downregulated HECTD1 protein expression. Furthermore, in vitro assays demonstrated that the upregulation of circHECTD1 inhibited the activation and migration of fibroblasts.

It has been confirmed that circRNA can play a role in the adsorption of miRNA and compete for miRNA binding sites, thereby reducing the ability of targeted mRNA expression. Part of the circRNA, including the open reading frame, can be translated into functional proteins. It is also speculated that circRNA can bind, store, and sort proteins to specific subcellular locations, and participate in protein interactions as a dynamic regulator. circRNA can enhance the expression of parent genes; circRNA can also regulate the expression of parental

genes via interaction with U1 snRNP and Pol II.[48] Many circRNAs are predicted to interact with RNA binding proteins (RBPs), such as quaking (QKI) and muscleblind (MBL), which have been reported to play a role in circRNA biogenesis. QKI increases circRNA numbers and abundance and promotes circRNA biogenesis during EMT.[49–51] However, the expression of QKI-5 increased after SiO_2 exposure (Figure S6a,b), combined with a decrease in circHECTD1, ruling out the role of RBPs and indicating that circHECTD1 may regulate the protein level of its host gene, *Hectd1*, through competition with its pre-mRNA, although further experiments are required.

Although this study still focused on the classical pathophysiology of pulmonary fibrosis, it provided new ideas to treat silicosis. Recently, there have been an increasing number of new ideas to cure pulmonary fibrosis. Based on previous studies, we found that the formation and development of pulmonary fibrosis are related to cell senescence, which is caused by telomere attrition, genomic instability, and loss of proteostasis.[52] circRNAs are specifically reported to modulate the cell cycle; moreover, their closed loop structure has high stability. HECTD1 is an E3 ubiquitin ligase that is associated with the regulation of the unfolded protein response, eliminating abnormal proteins to repair organelle damage.[53] Many proteins have been demonstrated to be able to promote cell regeneration and differentiation to inhibit fibrosis and repair cell damage. Combined with the ability of HECTD1 to accelerate proliferation, we think this might represent a potential therapeutic approach for pulmonary fibrosis.

In summary, our study indicated that HECTD1 is a crucial protein in silicosis, and is involved in multiple vital cell functions, such as autophagy, activation, and migration. circHECTD1 could regulate HECTD1 and might act as a predicted biomarker for silicosis. Additionally, the expression of circHECTD1/HECTD1 is related to the regulation of the progression of pulmonary fibrosis. circHECTD1/HECTD1 thus provides a new way to explore the pathogenesis of silicosis and might be a potential therapeutic target for silicosis.

Conclusion

Our study suggests that HECTD1-mediated fibroblast activation induced by SiO_2 and circHECTD1 could regulate fibroblast activation and migration by influencing the expression of HECTD1. Therefore, targeting circHECTD1/HECTD1-mediated autophagic signaling provides a potential therapeutic strategy for treating silicosis.

Acknowledgements

Authors Han Chu, Wei Wang, Wei Luo, and Wei Zhang contributed equally.

Author contributions

HC, WW, WL, and WZ performed the experiments, interpreted the data, prepared the figures, and wrote the manuscript. JH, YC, JW, XD, and SF performed the experiments and interpreted the data. JC provided laboratory space and funding, designed the experiments, interpreted the data, wrote the manuscript, and directed the project. All authors read, discussed, and approved the final manuscript.

Funding

The author(s) disclosed receipt of the following financial support for the research, authorship, and publication of this article: This work was supported by the National Natural Science Foundation of China (grant numbers 81972987, 81773796, 81700068, 81803182, and 81600045) and National Key R&D Program of China (grant number 2017YFA0104303).

Conflict of interest statement

The author(s) declared no potential conflicts of interest with respect to the research, authorship, and/or publication of this article.

ORCID iD

Jie Chao https://orcid.org/0000-0002-7800-3557

Supplemental material

Supplemental material for this article is available online.

References

1. Leung CC, Yu IT and Chen W. Silicosis. *Lancet* 2012; 379: 2008–2018.
2. Verma DK, Ritchie AC and Muir DC. Dust content of lungs and its relationships to pathology, radiology and occupational exposure in Ontario hardrock miners. *Am J Ind Med* 2008; 51: 524–531.
3. Steenland K and Ward E. Silica: a lung carcinogen. *CA Cancer J Clin* 2014; 64: 63–69.

4. Miao R, Ding B, Zhang Y, *et al*. Proteomic profiling change during the early development of silicosis disease. *J Thorac Dis* 2016; 8: 329–341.
5. Hamilton Jr RF, Thakur SA and Holian A. Silica binding and toxicity in alveolar macrophages. *Free Radic Biol Med* 2008; 44: 1246–1258.
6. McCabe Jr MJ. Mechanisms and consequences of silica-induced apoptosis. *Toxicol Sci* 2003; 76: 1–2.
7. Liu X, Fang S, Liu H, *et al*. Role of human pulmonary fibroblast-derived MCP-1 in cell activation and migration in experimental silicosis. *Toxicol Appl Pharmacol* 2015; 288: 152–160.
8. Liu H, Dai X, Cheng Y, *et al*. MCPIP1 mediates silica-induced cell migration in human pulmonary fibroblasts. *Am J Physiol Lung Cell Mol Physiol* 2016; 310: L121–L132.
9. Liu H, Cheng Y, Yang J, *et al*. BBC3 in macrophages promoted pulmonary fibrosis development through inducing autophagy during silicosis. *Cell Death Dis* 2017; 8: e2657.
10. Zhou Z, Jiang R, Yang X, *et al*. circRNA mediates silica-induced macrophage activation via HECTD1/ZC3H12A-dependent ubiquitination. *Theranostics* 2018; 8: 575–592.
11. White E, Mehnert JM and Chan CS. Autophagy, metabolism, and cancer. *Clin Cancer Res* 2015; 21: 5037–5046.
12. Iwata JI, Ezaki J, Komatsu M, *et al*. Excess peroxisomes are degraded by autophagic machinery in mammals. *J Biol Chem* 2006; 281: 4035–4041.
13. Shimizu Y, Dobashi K, Nagase H, *et al*. Co-localization of iron binding on silica with p62/sequestosome1 (SQSTM1) in lung granulomas of mice with acute silicosis. *J Clin Biochem Nutr* 2015; 56: 74–83.
14. Levine B, Mizushima N and Virgin HW. Autophagy in immunity and inflammation. *Nature* 2011; 469: 323–335.
15. Matsuzawa-Ishimoto Y, Hwang S and Cadwell K. Autophagy and inflammation. *Annu Rev Immunol* 2018; 36: 73–101.
16. Liu H, Fang S, Wang W, *et al*. Macrophage-derived MCPIP1 mediates silica-induced pulmonary fibrosis via autophagy. *Part Fibre Toxicol* 2016; 13: 55.
17. Memczak S, Jens M, Elefsinioti A, *et al*. Circular RNAs are a large class of animal RNAs with regulatory potency. *Nature* 2013; 495: 333–338.
18. Chen LL and Yang L. Regulation of circRNA biogenesis. *RNA Biol* 2015; 12: 381–388.
19. Huang C and Shan G. What happens at or after transcription: insights into circRNA biogenesis and function. *Transcription* 2015; 6: 61–64.
20. Hansen TB, Jensen TI, Clausen BH, *et al*. Natural RNA circles function as efficient microRNA sponges. *Nature* 2013; 495: 384–388.
21. Du WW, Yang W, Liu E, *et al*. Foxo3 circular RNA retards cell cycle progression via forming ternary complexes with p21 and CDK2. *Nucleic Acids Res* 2016; 44: 2846–2858.
22. Pamudurti NR, Bartok O, Jens M, *et al*. Translation of circRNAs. *Mol Cell* 2017; 66: 9–21.e7.
23. Huang MS, Zhu T, Li L, *et al*. LncRNAs and CircRNAs from the same gene: masterpieces of RNA splicing. *Cancer Lett* 2018; 415: 49–57.
24. Zohn IE, Anderson KV and Niswander L. The Hectd1 ubiquitin ligase is required for development of the head mesenchyme and neural tube closure. *Dev Biol* 2007; 306: 208–221.
25. Chen L, Luo W, Zhang W, *et al*. circDLPAG4/HECTD1 mediates ischaemia/reperfusion injury in endothelial cells via ER stress. *RNA Biol* 2019; DOI: 10.1080/15476286.2019.1676114.
26. Duhamel S, Goyette MA, Thibault MP, *et al*. The E3 ubiquitin ligase HectD1 suppresses EMT and metastasis by targeting the +TIP ACF7 for degradation. *Cell Rep* 2018; 22: 1016–1030.
27. Aleidi SM, Yang A, Sharpe LJ, *et al*. The E3 ubiquitin ligase, HECTD1, is involved in ABCA1-mediated cholesterol export from macrophages. *Biochim Biophys Acta* 2018; 1863: 359–368.
28. Li X, Zhou Q, Sunkara M, *et al*. Ubiquitylation of phosphatidylinositol 4-phosphate 5-kinase type I gamma by HECTD1 regulates focal adhesion dynamics and cell migration. *J Cell Sci* 2013; 126: 2617–2628.
29. Huang R, Zhang Y, Han B, *et al*. Circular RNA HIPK2 regulates astrocyte activation via cooperation of autophagy and ER stress by targeting MIR124–2HG. *Autophagy* 2017; 13: 1722–1741.
30. Wang W, Liu H, Dai X, *et al*. p53/PUMA expression in human pulmonary fibroblasts mediates cell activation and migration in silicosis. *Sci Rep* 2015; 5: 16900.
31. Pollard KM. Silica, silicosis, and autoimmunity. *Front Immunol* 2016; 7: 97.

32. Hanawa H, Abe S, Hayashi M, *et al.*, Time course of gene expression in rat experimental autoimmune myocarditis. *Clin Sci* 2002; 103: 623–632.

33. Keogh BA and Crystal RG. Alveolitis: the key to the interstitial lung disorders. *Thorax* 1982; 37: 1–10.

34. Ward PA and Hunninghake GW. Lung inflammation and fibrosis. *Am J Respir Crit Care Med* 1998; 157: S123–S129.

35. Ren Z, Hou Y, Ma S, *et al*. Effects of CCN3 on fibroblast proliferation, apoptosis and extracellular matrix production. *Int J Mol Med* 2014; 33: 1607–1612.

36. Wang P, Zhao F, Nie X, *et al*. Knockdown of NUP160 inhibits cell proliferation, induces apoptosis, autophagy and cell migration, and alters the expression and localization of podocyte associated molecules in mouse podocytes. *Gene* 2018; 664: 12–21.

37. Zhu T, Yao Q, Wang W, *et al*. iNOS induces vascular endothelial cell migration and apoptosis via autophagy in ischemia/reperfusion injury. *Cell Physiol Biochem* 2016; 38: 1575–1588.

38. Fang S, Guo H, Cheng Y, *et al*. circHECTD1 promotes the silica-induced pulmonary endothelial–mesenchymal transition via HECTD1. *Cell Death Dis* 2018; 9: 396.

39. Li X, Zhou Q, Sunkara M, *et al*. Ubiquitylation of phosphatidylinositol 4-phosphate 5-kinase type I by HECTD1 regulates focal adhesion dynamics and cell migration. *J Cell Sci* 2013; 126: 2617–2628.

40. Sarkar AA and Zohn IE. Hectd1 regulates intracellular localization and secretion of Hsp90 to control cellular behavior of the cranial mesenchyme. *J Cell Biol* 2012; 196: 789–800.

41. Del Valle PR, Milani C, Brentani MM, *et al*. Transcriptional profile of fibroblasts obtained from the primary site, lymph node and bone marrow of breast cancer patients. *Genet Mol Biol* 2014; 37: 480–489.

42. Fang S, Guo H, Cheng Y, *et al*. circHECTD1 promotes the silica-induced pulmonary endothelial-mesenchymal transition via HECTD1. *Cell Death Dis* 2018; 9: 396.

43. Li Z, Huang C, Bao C, *et al*. Exon-intron circular RNAs regulate transcription in the nucleus. *Nat Struct Mol Biol* 2015; 22: 256–264.

44. Yang ZG, Awan FM, Du WW, *et al*. The circular RNA interacts with STAT3, increasing its nuclear translocation and wound repair by modulating Dnmt3a and miR-17 function. *Mol Ther* 2017; 25: 2062–2074.

45. Jeck WR and Sharpless NE. Detecting and characterizing circular RNAs. *Nat Biotechnol* 2014; 32: 453–461.

46. Guo JU, Agarwal V, Guo H, *et al*. Expanded identification and characterization of mammalian circular RNAs. *Genome Biol* 2014; 15: 409.

47. Legnini I, Di Timoteo G, Rossi F, *et al*. Circ-ZNF609 is a circular RNA that can be translated and functions in myogenesis. *Mol Cell* 2017; 66: 22–37.e9.

48. Cortés-López M and Miura P. Emerging functions of circular RNAs. *Yale J Biol Med* 2016; 89: 527–537.

49. Hayakawa-Yano Y, Suyama S, Nogami M, *et al*. An RNA-binding protein, Qki5, regulates embryonic neural stem cells through pre-mRNA processing in cell adhesion signaling. *Genes Dev* 2017; 31: 1910–1925.

50. Conn SJ, Pillman KA, Toubia J, *et al*. The RNA binding protein quaking regulates formation of circRNAs. *Cell* 2015; 160: 1125–1134.

51. van der Veer EP, de Bruin RG, Kraaijeveld AO, *et al*. Quaking, an RNA-binding protein, is a critical regulator of vascular smooth muscle cell phenotype. *Circ Res* 2013; 113: 1065–1075.

52. López-Otín C, Blasco MA, Partridge L, *et al*. The hallmarks of aging. *Cell* 2013; 153: 1194–1217.

53. Deng S and Huang C. E3 ubiquitin ligases in regulating stress fiber, lamellipodium, and focal adhesion dynamics. *Cell Adh Migr* 2014; 8: 49–54.